Adaptive Lidar Signal Processing to Study the Diurnal Cycles of Atmospheric Boundary Layer Dynamics, Wind and Turbulence in Urban Environments

Mark Arend(a), Morann Dagan(a), Ivan Valerio(a), Sameh Abdelazim(b)
Fred Moshary(a)

(a) Department of Electrical Engineering City College of New York and NOAA CREST CUNY
New York, NY 10031
(b) School of Computer Sciences and Engineering, Fairleigh Dickinson University
Lead Author e-mail address: marend@ccny.cuny.edu

Abstract: Fiber optic based (1.5 micron) lidar technologies have been used to produce both a coherent Doppler lidar (CDL) system and a direct detection lidar (DDL) system. Special attention has been afforded in the design of the CDL system to allow for adaptive signal processing of both the accumulated correlograms and the power spectra. Both the CDL and the DDL systems require adaptive signal processing in order to account for baseline drifts that are due to both systematic changes in the operating conditions as well as dynamic changes in atmospheric boundary layer. Co-operating these two systems together (along with other meteorological profilers) has opened up opportunities to improve the vertical profiling of, wind, turbulent kinetic energy, water vapor, humidity and temperature in urban environments where diurnal cycles are often observed.

Keywords: Doppler lidar, Wind Profiler, Fiber Optics, Turbulence, Atmospheric Boundary Layer, Urban Meteorology

1. Introduction

The study of urban atmospheric boundary layer dynamics and turbulence by use of ground based profiling instrumentation provides valuable information that can be used for making decisions that affect many aspects of society (e.g. energy security, public health and safety, transportation, agriculture) as highlighted by the National Academies Press [1,2]. However, defining turbulence and deriving closed form physical solutions that are based on strict axiomatic and physical principles continues to challenge fundamental mathematical formalisms that rely on assumptions that are inherent in continuum mechanics and kinetic theory [3]. Such a challenge has inspired the continued development of fundamental theories that attempt to skirt the necessity of the Navier Stokes equation and the Boltzmann equation in order to formulate the principles of and to provide solutions to the time evolution of hydro dynamic systems [4]. Experiments that challenge and/or support these theories by providing precise multi sensor observations may discover the subtleties of such a complex system. To that end, the ability to experimentally characterize urban atmospheric boundary layer dynamics with instrumentation that both accounts for systematic drifts and fluctuations and is also capable of anticipating and adapting to changes that arise from the tempestuous nature of the atmosphere, provides a platform for which practical applications and fundamental research can be simultaneously explored. The design, operation and results of a fiber based coherent detection lidar system and a fiber based direct detection lidar system will be described in this report along with their relationships to other boundary layer monitoring instruments, specifically a microwave radiometer.

2. Instrument descriptions and analysis methods:

Coherent detection Doppler lidar. The system [5] consists of a 1542 nm CW laser fiber laser that is split in to two paths such that one path is used for a local oscillator and the other path is amplified by a single mode erbium doped fiber amplifier EDF and then modulated by an acousto-optic modulator, producing 200 nsec pulses at 20 kHz. These pulses are amplified further with a final amplifier and sent to an optical circulator before being launched in to the 4 inch clear aperture telescope from the single mode fiber. The aerosol back scattered light from the atmosphere is gathered by the telescope, passed through the circulator and mixed with the local oscillator with a 2x2 coupler. A 120 MHZ bandwidth balanced photodetector followed by TIA amplifiers detect the signal which is then sampled by a 400 MS/sec 12 bit ADC. These signals are processed with a FPGA that calculates gated Fourier transforms (or autocorrelations depending on the chosen mode [6]) and accumulate power spectra for further processing on a host computer using a maximum likelihood estimation method. **Systematic and adaptive processing to account for baseline drifts and background:** The spectral gain shape characteristics of the receiver system is not necessarily flat but the spectral response can be measured by operating the system with the final amplifier turned off. Depending on the required sensitivity and integration times, it pays to occasionally monitor the spectral response due systematic component drifts that are sometimes less than fraction of a dB. In addition, monitoring range gates that are far from the lidar transceiver (up to 7.5 km for a 20 kHz rep rate system) offers real time corrections to the spectral flattening process but again, depending on the sensitivity requirements and integration times, atmospheric processes can contribute to slight variations of these baseline measurements. Even though the narrow bandwidth aerosol back scatter component is dominant, it is the wide band width molecular backscatter component that influences this baseline measurement and opens up the possibility to monitor temperature profiles by appropriately accounting for these baseline drifts.

Direct detection lidar: The system runs with two channels at wavelengths of 1.545 µm (6472.5 cm-1) and at 4.55 µm (2197.8 cm-1). The 1.545 µm laser source is a 20 kHz Keopsys fiber laser with a peak power of 4 kW and pulse width of 7 ns (30 µJ/pulse). The laser source for the 4.55 µm channel is a 100 kHz Pranalytica Inc. QC laser which can deliver a peak power of 4.5 watts with a pulse width of 202 ns (0.9 µJ/pulse). Quantum-Cascade lasers offer several Watts of pulsed peak optical power, while retaining a good far field pattern as required for laser remote sensing techniques in atmospheric research. Mid-IR QC lasers produce pulsed signal at room temperature and are compact in size. The receiver consists of an f/3 10" primary mirror with a focal length of 762 mm focusing on a Vigo PVI-4TE-5 detector for the 4.55 µm channel and a Thorlabs APD110C for the 1.545 µm channel. The signal is then recorded by a 16 bit Gage digitizer with an onboard FPGA card for a maximum of 1024 hardware averages. This acquisition system has a maximum sampling rate of 200 MS/s. The dual channel IR lidar was designed to be light and compact, weighing less than 30 lbs; therefore making it portable. **Systematic and adaptive processing to account for baseline drifts and background:** The background data is considered here as the noise at the end of the signal where there is no aerosol signal; data points taken from the higher altitudes passed the PBL. To remove the background from each data set, we take the average of several data points at a high altitude and where there is no backscattered signal from aerosol or cloud and subtract it out from that data set; basically removing the DC value. The baseline for this system configuration is considered as data collected with all instruments in the system turned on, except for the laser which is turned off. The baseline gives information about the system instrumental noise including any features caused by any device. The baseline of the system is important to understand so that unusual features from instruments won't be mistaken for signal or overpower the signal.

Microwave Radiometer: The MP-3000A incorporates two radio frequency (RF) subsystems in the same cabinet. These RF subsystems share the same antenna and antenna pointing system. The temperature profiling subsystem utilizes sky brightness temperature observations at selected frequencies between 51 and 59 GHz. Although not presented here, this instrument also measures the vertical profile of temperature, humidity and liquid water content and is being used to characterize atmospheric stability [7].

3. Coherent Lidar Co-operated with Direct Detection Lidar

Co-operating the coherent Doppler lidar system alongside the direct Doppler lidar system can expose the dynamics of the boundary layer. A particular example corresponding to a short time of operation in the early evening (between about 5 pm and 6:40 pm) on August 25, 2015 is shown in Fig. 1.

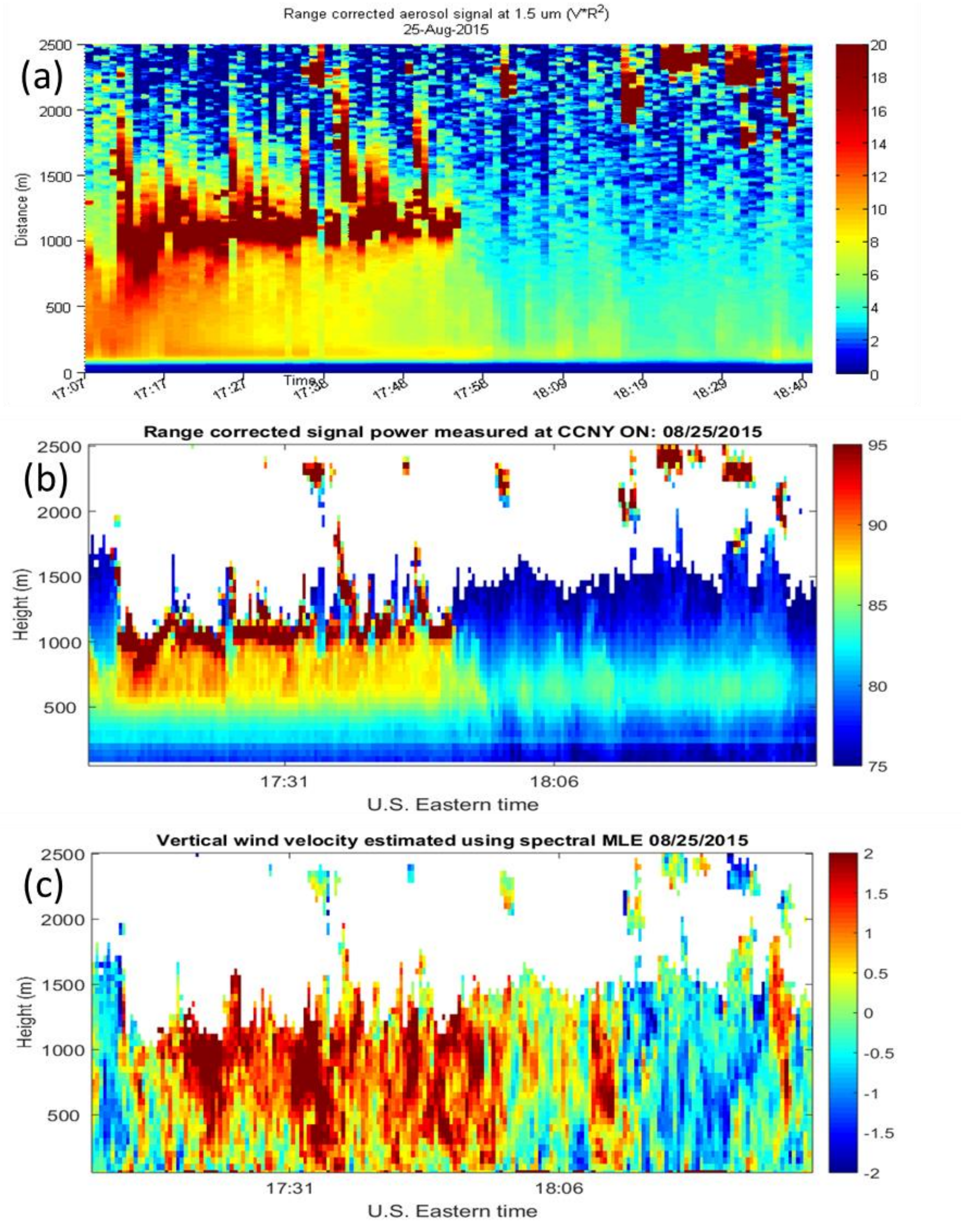

Figure 1. Vertical profile of the normalized range corrected signal for the direct detection (a) and coherent detection lidar and the vertical velocity component (c) in m/s on 8/25/2015 in upper Manhatten.

During this particular event, a dense cloud cover was associated with a strong updraft in the earlier half of the period and then as the clouds cleared out in the latter half of the time period. In the later part of the event, a cyclic behavior of aerosol concentration and clouds is observed by both lidars. A slight unexplained discrepancy of the vertical distribution of the aerosol concentration is observed when comparing both lidars in the later part of the event.

4. Coherent Lidar Co-operated with Microwave Radiometer

Diurnal patterns of atmospheric stability are being investigated with the suite of instruments that make up the NYCMetNet [2, 7]. An example of the use of the Doppler lidar in co-operation with the microwave radiometer is shown in Fig 2. These plots represent a period of about 39 hour starting at about 9 am in the morning on July 2nd, 2015. On these two days, a clear diurnal pattern of changes in the thermal gradient is observed by the microwave radiometer. The Doppler lidar observes a remarkable pattern that is coincident with this thermal gradient pattern that shows strong turbulent fluctuations occurring during periods in which the thermal gradient changes.

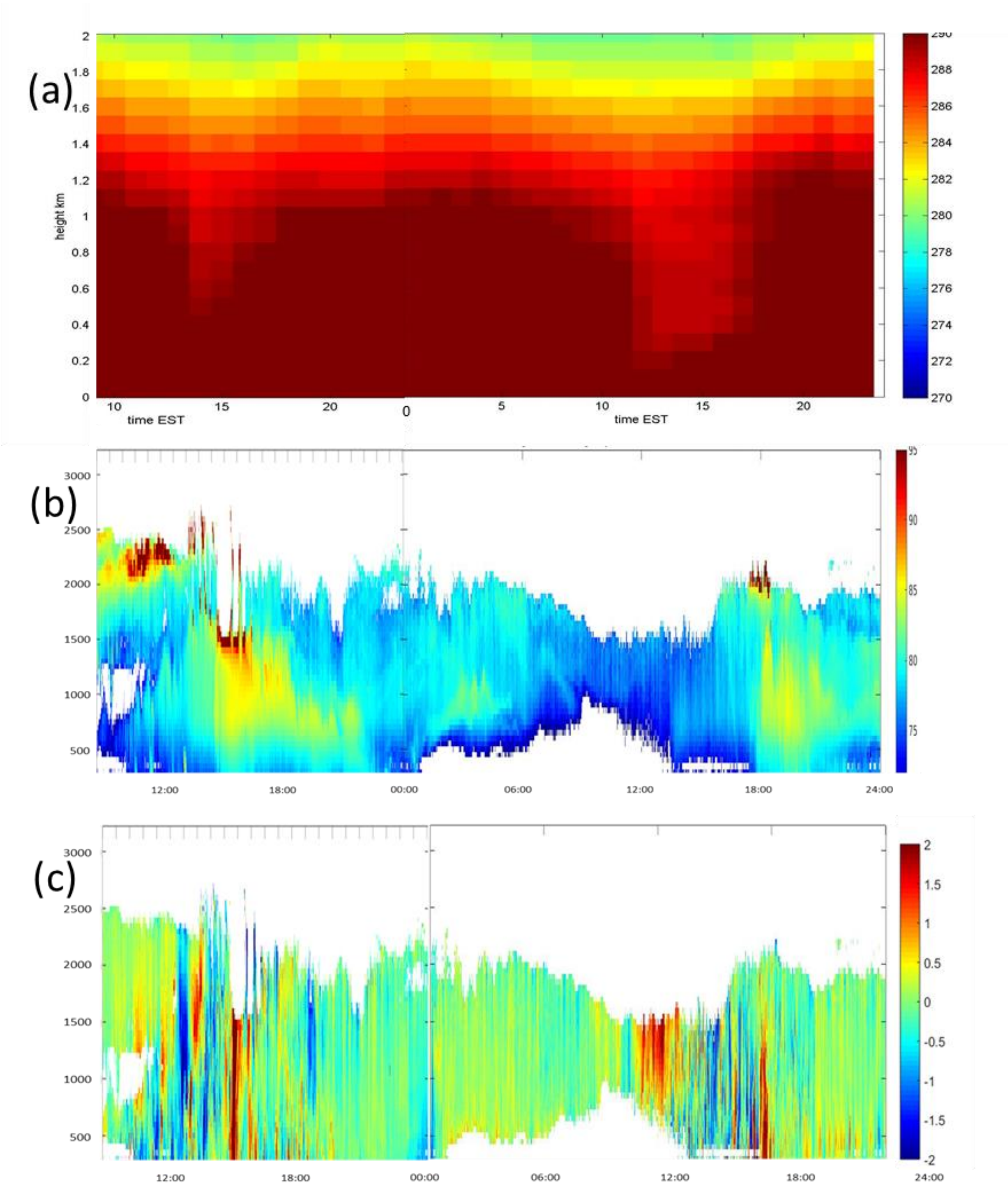

Figure 2. (a) Microwave radiometer temperature profuile, (b) Range corrected normalized Doppler lidar signal and (c) vertical velocity (m/s) during July 2nd and July 3rd, 2015.

[1] National Research Council. *Observing Weather and Climate from the Ground Up: A Nationwide Network of Networks*. Washington, DC: The National Academies Press, 2009. doi:10.17226/12540.

[2] Arend, M., 2012, NYCMetNet Graphic, in Urban Meteorology: Forecasting, Monitoring, and Meeting Users' Needs, Board on Atmospheric Sciences and Climate, National Academy of Sciences, NRC, National Academies Press, Washington. pg. 54, http://www.nap.edu/openbook.php?record_id=13328&page=54

[3] Gorban A.N.; Karlin, I. "Hilbert's 6th Problem: Exact and Approximate Hydrodynamic Manifolds for Kinetic Equations" Bull. Amer. Math. Soc. 51 (2014), 187-246

[4] Muriel, A. (2015). Time evolution equations for hydrodynamic variables with arbitrary initial data. Results in Physics.

[5] Abdelazim, S., Santoro, D., Arend, M., Moshary F., and Ahmed, S., "Development and Operational Analysis of an All-Fiber Coherent Doppler Lidar System for Wind Sensing and Aerosol Profiling," *IEEE TRANSACTIONS ON GEOSCIENCE AND REMOTE SENSING*, vol. 73, no. 12, pp. 6495 - 6506, 2015.

[6] Arend, M., Abdelazim, S., Lopez, M., and Moshary, F., (2013) "A comparison of two embedded programming techniques for high rep rate coherent Doppler lidars," Proc. SPIE 8731, Laser Radar Technology and Applications XVIII, 87310E (28 May 2013); doi: 10.1117/12.2016018

[7] Melecio-Vázquez, D., González-Cruz, J., Arend, M., Han, Z., , Dempsey, M., , Booth. B., Gutierrez, E.,, "New York Metro-Area Boundary Layer Catalogue: Boundary Layer Height and Stability Conditions from Long-Term Observations", 9th International Conference on the Urban Climate, 2015, Toulouse, France